Supplementary information

Table S1. Antibodies

Antibody	Fluorochrome	Clone	Supplier	Catalogue number	Dilution
CD5	Biotin		Biolegend	100603	1:250
CD49b	Biotin		eBioscience	13-0491-85	1:250
CD45R (B220)	Biotin		Biolegend	103203	1:250
CD117	Biotin		Biolegend	105803	1:250
F4/80	Biotin		Biolegend	123105	1:250
TER119	Biotin		Biolegend	116204	1:250
CD3	APC/Cy7	17A2	Biolegend	100221	1:100
CD19	PE	6D5	Biolegend	115507	1:100
CD18	PE	M18/2	Biolegend	101408	1:100
CD29	APC	HMß1-1	Biolegend	303003	1:100
CD45.2	PerCP/Cy5.5	104	BD	552950	1:100
Ly-4G/Ly-6C (Gr-1)	Pacific Blue	RB6-8C5	Biolegend	108430	1:100
F4/80	PerCP/Cy5.5	BM8	Biolegend	123127	1:100
F4/80	PE/Cy7	BM8	Biolegend	123113	1:100
Rat IgG2a, κ Isotype Ctrl	PE	RTK2758	Biolegend	400508	1:100
American Hamster IgG Isotype Ctrl	APC	HTK888	Biolegend	400912	1:100
Sytox®Blue			Life Technologies	S34857	1:3000
CD18 (LFA-1)	PerCP/Cy5.5	H155-78	Biolegend	141007	1:100
Rat IgG1, κ Isotype Ctrl	PerCP/Cy5.5	RTK2071	Biolegend	400425	1:100
VCAM1	PE	M/K-2	Invitrogen	RMCD10604	1:40
ICAM1	Alexa 488	YN1/1.7.4	Biolegend	116113	1:120
CD11b	Alexa 488	M1/70	eBioscience	53-0112-82	1:80

Table S2: Clinical characteristics of JAK2-V617F-positive or CALR-positive CMN patients.

UPN	Sex	Age	Diagnosis	mutation	JAK2-V617F allelic ratio
P1	male	51	ET	CALR (del52)	
P2	female	62	ET	CALR (del52)	
P3	male	71	ET	CALR (ins5)	
P4	male	53	PV	JAK-V617F	47.5
P5	female	77	ET	JAK-V617F	27.1
P6	male	66	PV	JAK-V617F	15.1

UPN – Unique Patient Number ET – Essential Thrombocythemia

PV – Polycythemia Vera

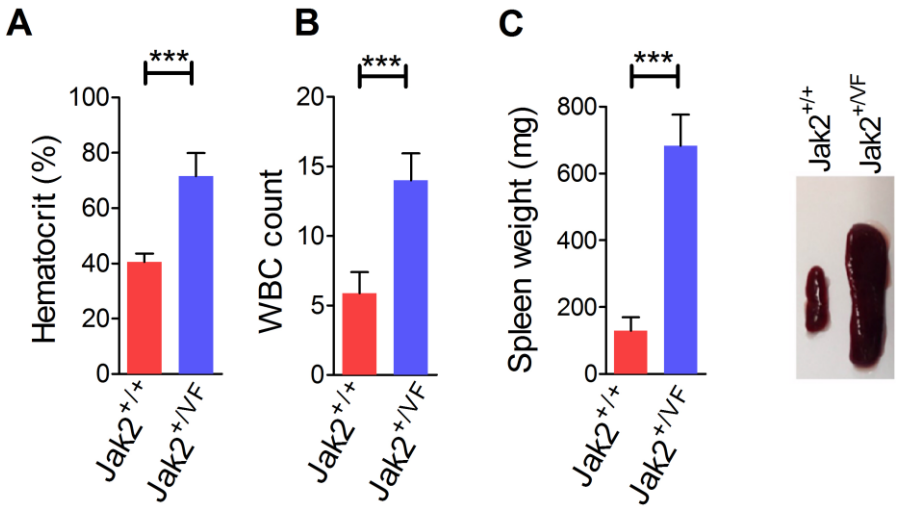

Supplemental Figure 1: Characterization of JAK2$^{+/VF}$ knock-in mice. Measurement of haematocrit (A), white blood cell (WBC) count (x 1000/ µL) (B) and spleen weight (C) of 10-12-week-old JAK2$^{+/+}$ (n = 10) and JAK2$^{+/VF}$ (n = 11) mice. A representative photograph of spleens from a JAK2$^{+/+}$ and a JAK2$^{+/VF}$ mouse are depicted in the right panel of (C). Data are shown as mean ± SEM.***$P \leq 0.001$ (unpaired, two-tailed Student`s *t* test).

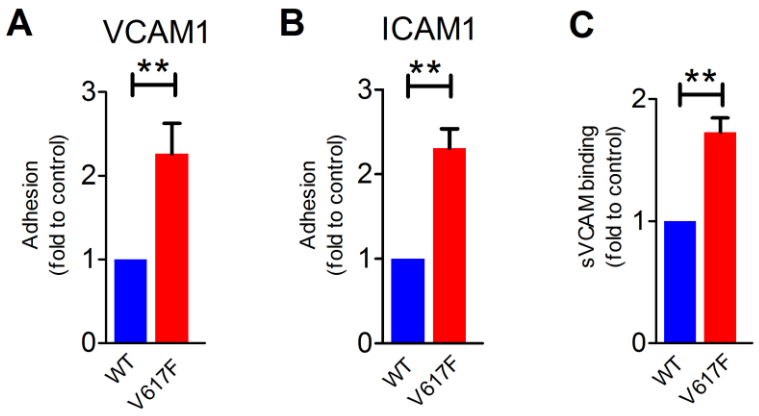

Supplemental Figure 2: Static adhesion and soluble ligand binding in BaF3 JAK2-WT and BaF3 JAK2-V617F cells. Static adhesion on Fc-free VCAM1 (A) and Fc-free ICAM1 (B) of BaF3 JAK2-WT (WT) and BaF3 JAK2-V617F (V617F) cells. (C) Soluble VCAM1 binding assay of BaF3 JAK2-WT and BaF3 JAK2-V617F cells. Data are shown as mean ± SEM. ***P* ≤ 0.01 (unpaired, two-tailed Student`s *t* test). Three independent experiments were performed each.

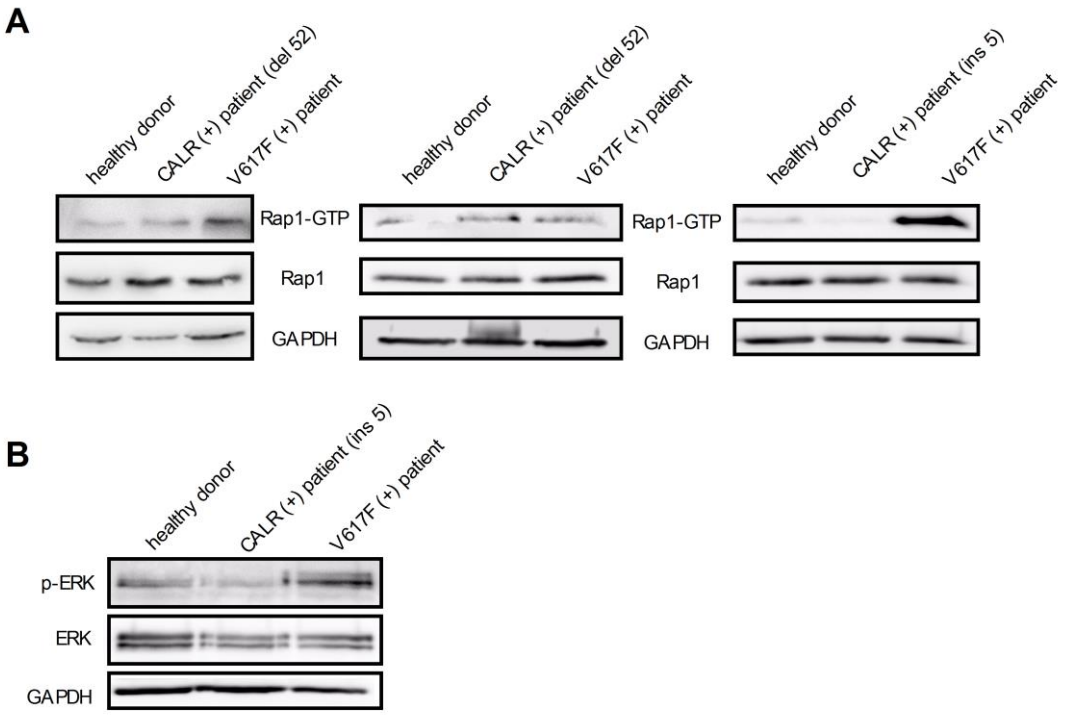

Supplemental Figure 3: Rap1 activation and ERK signaling in granulocytes from CALR positive patients as compared to JAK2-V617F mutated patients. (A) Rap1 is activated to a minor degree only in CALR positive human granulocytes. Western blot analysis of Rap1 activation of CALR positive patients (n = 3) compared to JAK2-V617F positive patients (n = 3) and healthy controls (n = 3). (B) Cellular lysates for additional signaling analysis were available in the CALR (ins5) mutated patient only. Depicted is Western blotting of ERK phosphorylation (phospho-p44/42 MAPK (Erk1/2) (Thr202/Tyr204)) in granulocytes of the CALR (ins5) mutated patient (n = 1) as compared to a JAK2-V617F positive patient (n =1) and a healthy control (n = 1). No phospho-protein signals were detectable for STAT5, JAK2 and Akt.

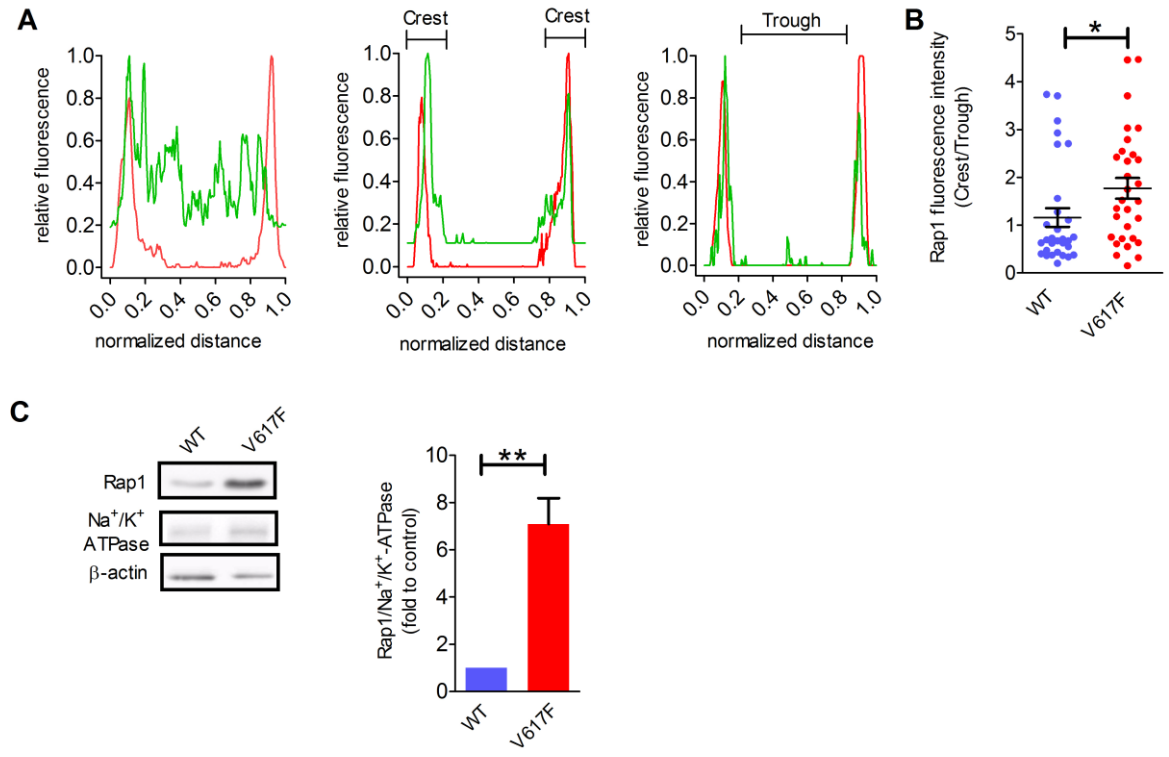

Supplemental Figure 4: Rap1 translocation towards the plasma membrane. (A) Line scan of Rap1 (green line) and actin (red line) fluorescence intensity in representative images from 32D JAK2-WT (left) and 32D JAK2-V617F (middle and right) cells. (B) Quantification of Rap1 fluorescence intensity following line-scan analysis. 30 random cells were analyzed from two independent experiments. Actin immunostaining was used to define the cell size, which in turn was determined by the length of the plotted line and was normalized between 0-1.0. The distance of 0-0.3 and 0.7-1.0 has been defined as ‘’crest’’ and between 0.4-0.6 as ‘’trough’’. The signal intensity of Rap1 was expressed as the ratio of crest and trough. Data shown as mean ± SEM. **P* ≤ 0.05, (unpaired, two-tailed Student`s *t* test). (C) Total membrane lysates obtained by subcellular fractionation of 32D JAK2-WT and 32D JAK2-V617F cells, respectively, were tested for Rap1. Na^+/K^+ ATPase immunoblotting was used to control enrichment in plasma membranes. β-actin immunoblotting was used as control for equal loading (left panel). Quantification of Rap1 in total membrane fractions of 32D JAK2-WT and V617F cells (right panel). Data shown as mean ± SEM. **P ≤ 0.01, (unpaired, two-tailed Student`s *t* test). Three independent experiments were performed each.

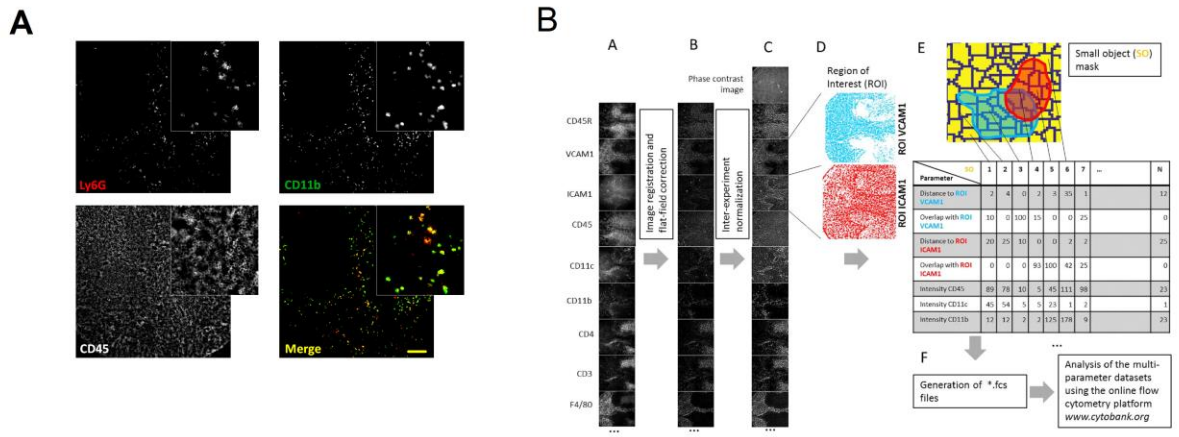

Supplemental Figure 5: Multi-epitope ligand cartography (MELC) image processing and data analysis. (A) Staining for CD11b and Ly6G. Merged image demonstrates that CD11b high positive cells ($CD11b^{++}$) are Ly6G positive. Scale bar corresponds to 100 µm; insert shows a size of 200 µm. (B) MELC image processing has been performed as described previously (51). Briefly, a series of raw fluorescence images acquired by the CCD camera of the MELC robot is shown (A). The corresponding phase contrast images (not all shown) were used to align all images of the series. Illumination fault due to the optics and the large CCD sensor were corrected using a flat-field image (selected from the series of post-bleach images). (B) The series of corrected fluorescence images from one single field of view is displayed. Fluorescent intensities had to be normalized due to variances during the sample preparation and variances in the staining efficiencies. (C) Fluorescence intensity images after inter-experiment normalization. (D) Regions of interest (ROI) are defined using an automated threshold based algorithm. (E) A mask of randomly distributed “small objects” (SO) of a size of 16 pixels is generated (yellow) of the given field of view. The minimal distances to the reference regions (e.g. VCAM1 in light blue or ICAM1 in red) or the pixel overlap can be determined for all SO. Arbitrary examples of these spatial data are shown in the first 4 rows of the table, whereas rows 5 to 7 show the mean fluorescent intensities of the markers for all SO. (F) Spatial data as well as the fluorescence data for all small objects were stored into FCS 3.0 data files, uploaded to the online multi-parameter flow cytometry data analysis platform www.cytobank.org.

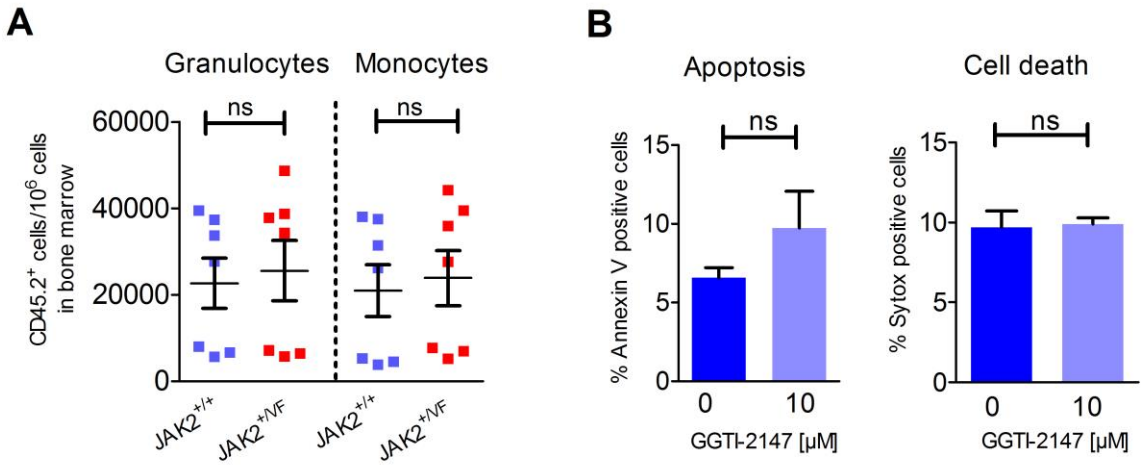

Supplemental Figure 6: In vivo homing assay. (A) Whole bone marrow (WBM) cells of 10-12-week-old $JAK2^{+/VF}$ or $JAK2^{+/+}$ mice (carrying the congenic marker CD45.2) were injected into CD45.1 recipient mice. 16 h after injection bone marrow of recipient mice was evaluated. Data represents the number of detected CD45.2-positive granulocytes and monocytes per 10^6 cells in the bone marrow (n = 7/group). (B) Flow cytometric measurement of apoptosis (left panel) and cell death (right panel) 16 h after treatment of murine bone marrow cells with GGTI-2147 (10 µM, 30 min); (-) indicates DMSO control.